Annals of Nuclear Medicine Vol. 10, No. 1, 153–160, 1996

Simulating technetium-99m cerebral perfusion studies with a three-dimensional Hoffman brain phantom: Collimator and filter selection in SPECT neuroimaging

Hee-Joung KIM,*,** Joel S. KARP,** P. David MOZLEY,** Seoung-Oh YANG,* Dae Hyuk MOON,* Hank F. KUNG,** Hee Kyung LEE* and Abass ALAVI**

*Department of Nuclear Medicine, University of Ulsan, Asan Medical Center
**Division of Nuclear Medicine, Department of Radiology, University of Pennsylvania

The choice of a collimator and the selection of a filter can affect the quality of clinical SPECT images of the brain. The compromises that 4 different collimators make between spatial resolution and sensitivity were studied by imaging a three-dimensional Hoffman brain phantom. The planar data were acquired with each collimator on a three-headed SPECT system and were reconstructed with both a standard Butterworth filter and a Wiener pre-filter. The reconstructed images were then evaluated by specialists in nuclear medicine and were also quantitatively analyzed with specific regions of interest (ROI) in the brain.

All observers preferred the Wiener filter reconstructed images regardless of the collimator used to acquire the planar images. With this filter, the ultrahigh-resolution fan-beam collimator was the most subjectively preferable and quantitatively produced the highest contrast ratios. The findings support suggestions that higher resolution collimators are preferable to higher sensitivity collimators, and indicate that fan-beam collimators are preferable to parallel-hole collimators for clinical SPECT studies of cerebral perfusion. The results also suggest that the Wiener filter enhances the quality of SPECT brain images regardless of which collimator is used to acquire the data.

Key words: SPECT, collimator, filter, neuroimaging

INTRODUCTION

SINGLE PHOTON EMISSION COMPUTED TOMOGRAPHY (SPECT) can be used to study regional cerebral perfusion in human brains with commercially available tracers such as [^{99m}Tc]HMPAO and [^{99m}Tc]ECD, and multi-headed SPECT camera.[1–3] The choice of a collimator and the selection of a filter can affect the quality of clinical SPECT images and ultimately influence the interpretability of the scans. SPECT image quality is directly dependent on spatial resolution and camera sensitivity, but resolution and sensitivity are often inversely related. A compromise between spatial resolution and sensitivity has been investigated by computer simulation with the Derenzo phantom[4] and by physical measurements with either the Jaszczak phantom or clinical studies.[5] Muehllehner[4] has studied these compromises with the simulated projection data by convolving the mathematical phantoms with a Gaussian function having a full width at half maximum (FWHM) appropriate for the detector response. The projection data in this studies were reconstructed with a filtered backprojection algorithm and ramp filters modified by a Hann window. Fahey et al. have extended Muehllehner's computer simulation studies with actually measured SPECT data.[5] They compared two sets of collimators provided with a commercially available three-headed SPECT camera (Trionix Research Laboratories, Twinsburg, OH): low-energy, high-resolution and low-energy, ultrahigh-resolution parallel-hole collimators. The measured projection data in their studies were reconstructed with a Hamming filter and a cutoff frequency of 1.0 Nyquist. Muehllehner and Fahey et al. concluded that higher resolution collimators are preferable to higher sensitivity collimators. In another example of simulation studies with a more realistic brain phantom,

Received May 17, 1995, revision accepted August 10, 1995.

For reprint contact: Hee-Joung Kim, Ph.D., Department of Nuclear Medicine, Asan Medical Center, 388–1 Poongnapdong, Songpaku, Seoul, KOREA.

E-mail: hjkim@soback.kornet.nm.kr

Madsen et al.[6] have indicated that the higher resolution should be preferable to the higher sensitivity collimators for [^{99m}Tc]-HMPAO perfusion studies.

Making physical measurements in phantoms filled with known amounts of radioactivity can help characterize and potentially quantify the effects of collimator design on SPECT images, but there have not been many comparison studies of the performance of the parallel hole and fan beam collimators. In addition, the effects of filter selection on different collimators have not been fully characterized with physically measured projection data and a realistic three-dimensional brain phantom.

We studied the performance of a three-headed Prism 3000 (Ohio Imaging of Picker International, Bedford Heights, Ohio) SPECT system equipped with 4 sets of collimators: low-energy, high-resolution parallel-hole (HRP), ultrahigh-resolution parallel-hole (UHRP), high-resolution fan-beam (HRF), and ultrahigh-resolution fan-beam (UHRF) collimators in imaging the brain. The HRF has been recommended for use in clinical neuroimaging protocols. The fan-beam collimators have the advantage of high sensitivity with almost the same resolution as the parallel-hole collimators.[7] In this paper, the compromises that 4 different collimators make between spatial resolution and sensitivity were studied by imaging a three-dimensional Hoffman brain phantom (Data Spectrum Inc., Hillsborough, N.C.). The effects of filter selection were also studied. For the qualitative data analysis, the observers test was used. The criteria were overall image quality and spatial resolution to determine how closely they can correlate the data with a bit map provided as a reference. For the quantitative data analysis, ROIs were drawn on a selected magnetic resonance image (MRI) at the level of the basal ganglia and overlaid onto the corresponding SPECT images. The ratios of activity (Gray/White, White/Ventricles, and Gray/Ventricles) for the collimators (HRF, UHRF, HRP, and UHRP) were compared.

MATERIALS AND METHODS

Modulation transfer function

The Wiener and Metz filters have previously been applied to partially correct for finite detector resolution, scatter, and septal penetration. These filters use the modulation transfer functions (MTFs) determined from the line spread functions (LSFs).[8–11] The MTFs used in this study were computed from the measured LSFs for each set of collimators. A line source (1 mm i.d., 22 cm length) centered in a cylindrical phantom (22 cm diameter, 22 cm length) was filled with ≈555 MBq (15 mCi) of [^{99m}Tc]. The cylindrical phantom was filled with water to simulate the scatter medium. The line source was imaged on a three-headed SPECT system (Prism 3000, Picker, Bedford Heights, Ohio) with each set of low-energy HRF, UHRF, HRP, and UHRP collimators. The acquisition parameters included a 14.5 cm rotational radius, a 20% energy window, and a 256 × 256 matrix with a pixel size of 1.78 mm. All experiments for this study were carried out with the same camera and similar acquisition parameters to those described here. The activity profile perpendicular to the line source, averaged over the full length of the line source but excluding the ends to avoid edge effects, was analyzed as the sum of three Gaussians[12] as follows:

$$\mathrm{LSF}(x) = \sum_i \mathrm{AMP}_i e^{-x^2/2\sigma_i^2} \qquad (1)$$

where LSF(x) is the line spread function in the spatial domain x, AMP$_i$ is the amplitude for i^{th} Gaussian, and σ_i is the standard deviation for i^{th} Gaussian. The first Gaussian represents the geometric detector response, while the second and third Gaussians represent the components due to scatter and septal penetration.[10,12,13] The MTFs used to generate the Wiener filters for these studies were obtained from the Fourier transformation[14,15] of the sum of three Gaussians as:

$$\mathrm{MTF}(u) = \frac{\int_{-\infty}^{\infty} \mathrm{LSF}(x) e^{-2\pi u x} dx}{\int_{-\infty}^{\infty} \mathrm{LSF}(x) dx} \qquad (2)$$

where MTF(u) is the normalized system MTF in the frequency domain u.

Tomographic spatial resolution and relative planar sensitivity

Tomographic images of the line source were acquired with each set of collimators in a 128 × 128 matrix with a pixel size of 3.56 mm. A step and shoot mode was used to obtain 120 angular views. The projection data were reconstructed with a ramp filter and the full width at the half maximum (FWHM) for each collimator was computed. The first projection data obtained from each head with a three-dimensional Hoffman brain phantom were summed and used to compute the relative planar sensitivity since each head was found to have a slightly different sensitivity. We used the first projection data for the brain phantom to compare relative sensitivities for different collimators for the Hoffman brain phantom.

Three-dimensional brain phantom measurements with SPECT and MRI

To quantify the effects of collimator and filter selection, magnetic resonance images (MRI) of the phantom were acquired on a 1.5 tesla scanner (GE Medical, Milwaukee, WI) with a repetition time (Tr) of 3,000 msec and an echo time (Te) of 80 msec. The phantom was imaged with and without a line source fixed to its surface to produce fiducial markers. The line source (1 mm i.d., 150 cm length) produced two markers on every slice in orthogonal planes (transaxial, coronal, and sagittal) (Fig. 1). The line source contained [Tc-99m] when the SPECT images were acquired, and [Cu-2 Acetate] when the MRI scans

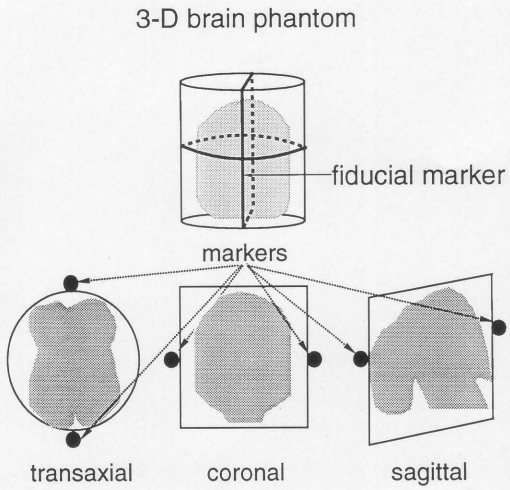

Fig. 1 Diagram of a three-dimensional brain phantom with a line source which allowed obtaining each slice with two markers in three orthogonal planes. Using these markers, the MRI and SPECT data were reformatted to obtain the same orientations and comparable slices. The fiducial marker was filled with [Tc-99m] for SPECT and [Cu-2 Acetate] for MRI.

were obtained. The three-dimensional Hoffman brain phantom[16] was filled with approximately 350 MBq (9.5 mCi) [^{99m}Tc] for the SPECT studies, and filled with water for the MRI studies. The projection data were acquired with each collimator for identical scanning times. The acquisition parameters were the same as described above for the tomographic line source measurements. The acquisition parameters were designed to simulate the ones that are used in clinical studies of cerebral perfusion. The images that were obtained with the fiducial markers in place were used to register the corresponding SPECT and MRI slices. The images obtained without the fiducial markers were then used in the quantitaive ROI data analysis to avoid spillover effects from the fiducial marker into the SPECT brain ROIs.

SPECT image reconstruction

The projection data for the three-dimensional brain phantom were reconstructed by means of both standard filtered back projection with a Butterworth filter with 3rd order and 0.14 cycles/pixel cutoff frequency, and a count-dependent Wiener filter.[8,17] The two-dimensional Wiener filter is defined as:

$$W(u,v) = \frac{MTF^2(u,v)}{MTF(u,v)[MTF^2(u,v) + N(u,v)/P(u,v)]} \quad (3)$$

where u and v are spatial frequencies, N is the noise power spectrum, P is the object power spectrum, and MTF is the modulation transfer function (MTF) that can be computed from the line spread function. The noise N was assumed to have a constant average value of its power spectrum equal to the total image count and the object power spectrum P was taken to be the image power spectrum minus the total count as reported by King et al.[17]

Chang's first order correction method[18] was used with an effective attenuation coefficient equal to 0.120 cm^{-1} [19,20] to compensate for the photon attenuation in the brain phantom. The published effective attenuation coefficient was used instead of the true attenuation coeffieient $\approx$0.150 cm^{-1} for Tc-99m since the true scatter correction was not applied in these studies.

DATA ANALYSIS

Observers test

The reconstructed images were evaluated by 6 nuclear medicine professionals who were unaware of how each image set was acquired and processed. The 4 sets of images processed with each filter were displayed simultaneously on a 21 inch monitor. The observers were then asked to rank the image sets in order from the most preferable to the least preferable. A bit map of the phantom was provided as a reference. The criteria were the noise characteristics related with system sensitivity; spatial resolution and structural integrity: how closely the reconstructed images corresponded to the bit map image in anatomical detail; and the image contrast between gray and white matter, gray and ventricles, and white matter and ventricles.

Semi-Quantitative ROI data analysis

The SPECT and MRI data obtained with the fiducial markers were used for selecting an identical slice at the level of the basal ganglia. With PETVIEW software, which combines image display and analysis, developed at the University of Pennsylvania, the SPECT and MRI data were reformatted to align them by rotating in three directions, transaxial, sagittal, and coronal. The external point markers in three directions were used for alignment. A representative slice was chosen by using an external hot ring at the level of the basal ganglia.[21] Regions of interest (ROI) containing 37 regions (22 for Gray (G), 8 for White (W), 6 for Ventricles (V) and 1 for whole brain) were drawn on a selected MRI slice at the level of the basal ganglia (Fig. 2A). The ROIs (Fig. 2B) were then overlaid with the corresponding SPECT data (Fig. 2C). Activity contrast ratios were computed for gray/white matter regions, white/ventricular regions and gray/ventricular regions.

RESULTS

SPECT Wiener filtering can partially compensate for the effects of the finite detector resolution, scatter, septal penetration, and statistical noise simultaneously, but the modulation transfer function (MTF) of the imaging system needs to be estimated accurately, and it is somewhat dependent on the object dimensions.

Plots of MTFs for HRF, UHRF, HRP and UHRP are

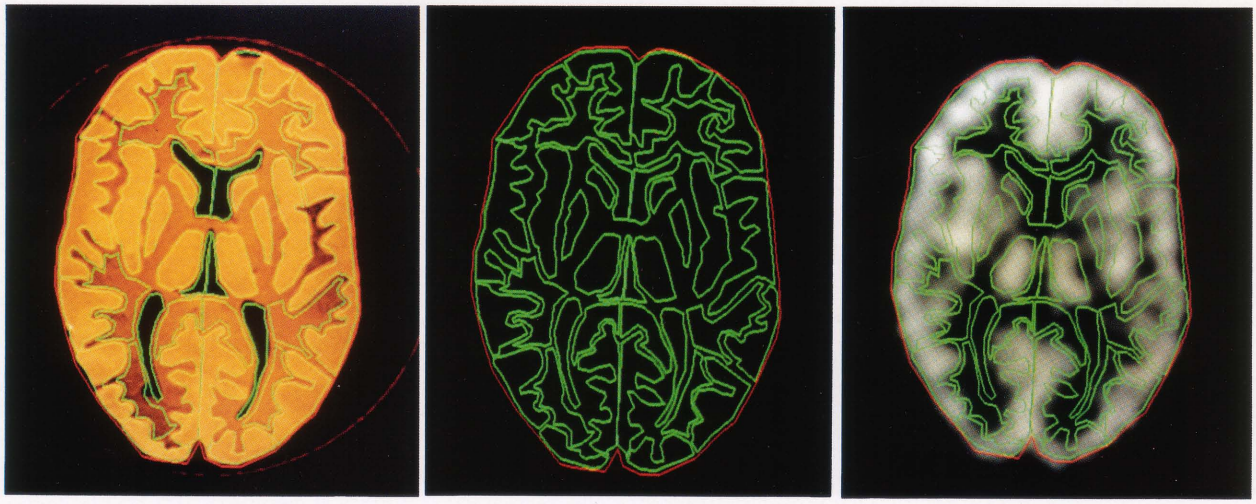

A B C

Fig. 2 Regions of interest (ROIs) containing 37 regions (22 for gray matter; 8 for white matter; 6 for ventricles; and 1 for whole brain) drawn on a selected MRI slice (A) and ROIs template alone (B) at the level of the basal ganglia. A typical example of a corresponding SPECT image overlaid with ROIs (C) to compute the ratios between the gray and white matter, the white matter and ventricles, and the gray matter and ventricles.

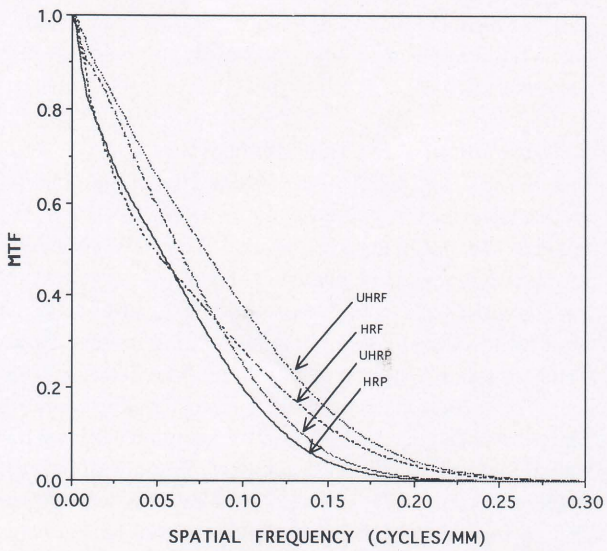

Fig. 3 Plots of system modulation transfer functions (MTFs) for a line source 14.5 cm from the face of the collimator and centered in the water-filled cylindrical phantom (22 cm diameter and 22 cm length). HRF, UHRF, HRP, UHRP denote high-resolution fan-beam, ultrahigh-resolution fan-beam, high-resolution parallel-hole, and ultra-high resolution parallel-hole collimators, respectively.

shown in Figure 3 for the 22 cm diameter cylindrical phantom. Both the parallel-hole and fan-beam ultra-high resolution collimators show less degradation in the MTFs than the corresponding high resolution (higher sensitivity) collimators. The parallel-hole collimators show more degradation in the MTFs, after the geometric magnification factor for fan-beam collimators has been accounted for. Tomographic spatial resolution and relative planar

Table 1 Tomographic spatial resolution and relative planar sensitivity

Collimator	Tomographic resolution (mm)	Relative planar sensitivity
HRP	11.7	0.68
UHRP	10.6	0.42
HRF	11.8	1.00
UHRF	9.8	0.52

sensitivity are summarized in Table 1. UHRF has the best resolution at 9.8 mm in the scattering medium (22 × 22 cm water-filled cylinder), while HRP and HRF have almost the same spatial resolution. The HRF has the best sensitivity, which is approximately 47% higher than the HRP. Three-dimensional brain phantom images reconstructed with a standard Butterworth filter (Fig. 4) or with a Wiener pre-filter (Fig. 5) for four different collimators are shown. The Wiener filter reconstructed images (Fig. 5) clearly show improvement over the Butterworth filtered backprojection reconstructed images (Fig. 4) for all of four different collimators. The Wiener filtered reconstructed images show better contrast between the gray and white matter and the gray matter and ventricles.

In the observers' test, all readers preferred the Wiener filter regardless of the collimator to the standard Butterworth filtered backprojection with order of 3 and cutoff frequency of 0.14 cycles/pixel. With this filter, the fractions preferring HRF, UHRF, HRP and UHRP were 0.33, 0.50, 0.00 and 0.17, respectively. These qualitative improvements are consistent with the quantitative improvements shown in Table 2. The Wiener prereconstruction filter significantly improves the image contrast (gray/

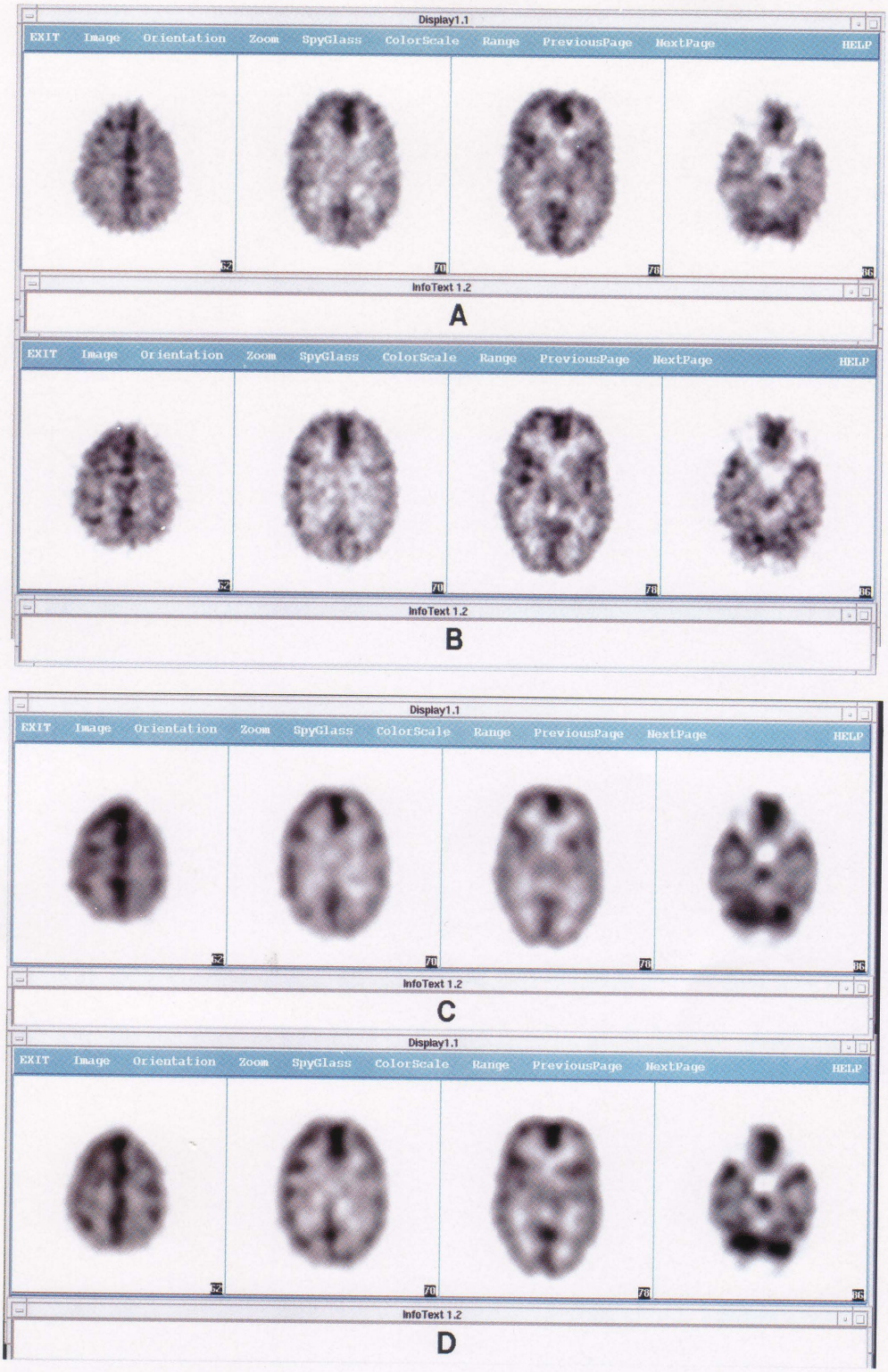

Fig. 4 Reconstructed images of a three-dimensional Hoffman brain phantom using filtered back projection with a Butterworth filter for four different collimators: low energy HRF (A), UHRF (B), HRP (C), and UHRP (D).

white matter, white matter/ventricles, and gray matter/ventricles) over the standard FBP for all four collimators. For example, the image contrast (gray/white matter) for the Wiener filtering (2.09/1) is closer to the true contrast (4/1) than is that for the standard FBP image contrast (1.37/1) for the HRF.

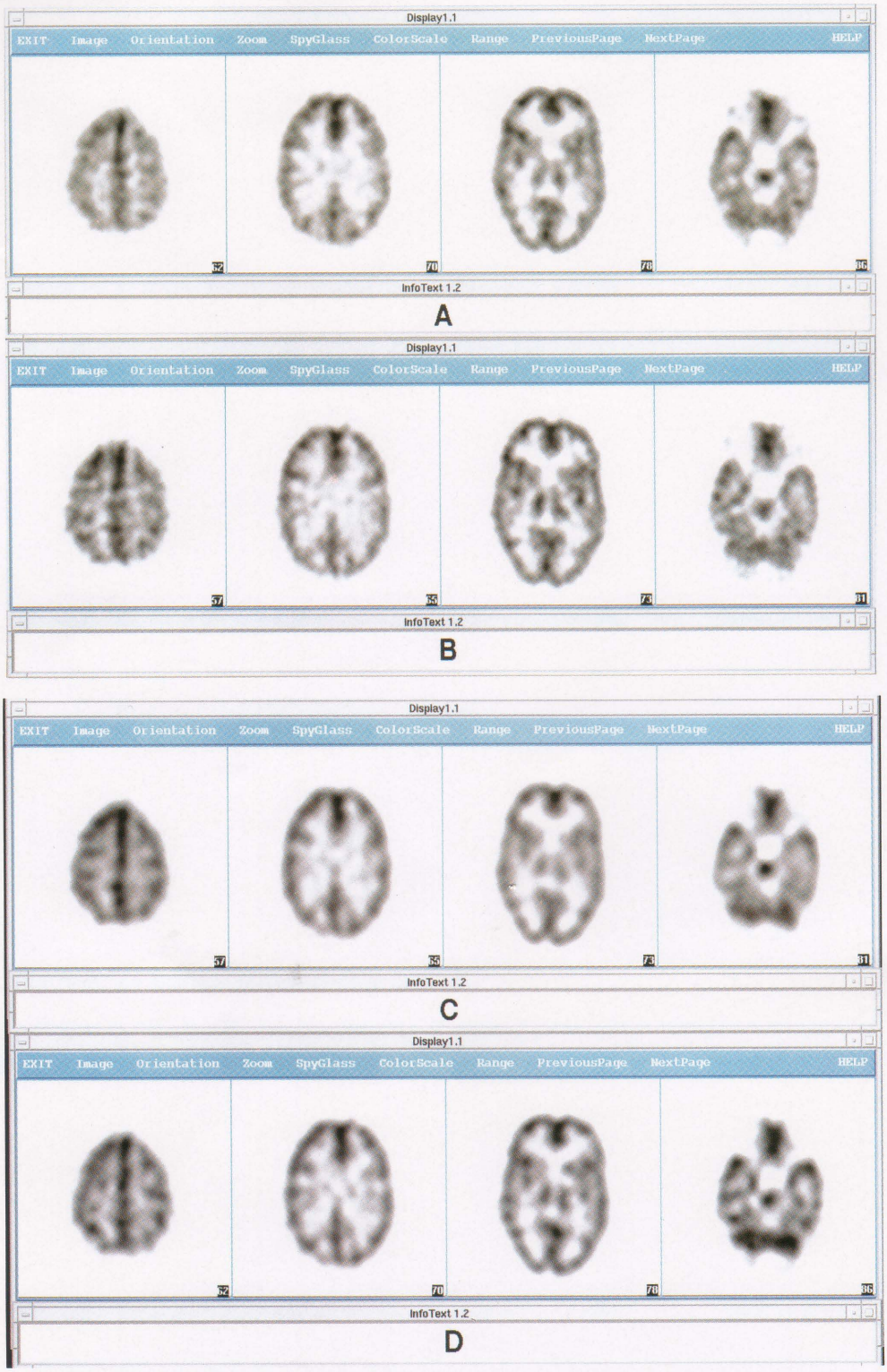

Fig. 5 Reconstructed images of a three-dimensional Hoffman brain phantom using a count dependent Wiener filter for four different collimators: low energy HRF (A), UHRF (B), HRP (C), and UHRP (D).

DISCUSSION

SPECT imaging is used frequently in various clinical settings to evaluate regional cerebral blood flow and function in patients with brain diseases. The choice of a collimator and the selection of a filter can affect the quality of clinical SPECT images of the brain. The compromises between resolution and sensitivity have been

Table 2 Ratios of gray/white, white/ventricles, and gray/ventricles for HRP, UHRP, HRF, and UHRF

Collimator	Gray/White		White/Ventricles		Gray/Ventricles	
	But	Wiener	But	Wiener	But	Wiener
HRP	1.35	1.90	1.26	1.74	1.71	3.31
UHRP	1.43	1.98	1.28	1.69	1.83	3.34
HRF	1.37	2.09	1.15	2.12	1.57	4.43
UHRF	1.49	2.18	1.29	1.34	1.92	4.65

investigated by using either simulated data[4] or measured data for parallel-hole collimators.[5] Most investigators have concluded that higher resolution collimators improve the image quality in SPECT studies in spite of decreased counting statistics due to the reduced collimator sensitivity. The HRF has frequently been used for imaging cerebral blood flow with the three-headed SPECT system. The HRF gives 47% higher sensitivity than the HRP with almost the same spatial resolution.

In the study described above, all readers preferred the Wiener filter to the Butterworth filter regardless of the collimator. For the Wiener filter, the UHRF was most preferable in image quality. In the ROI data analysis (Table 2), for both parallel-hole and fan-beam collimators, the higher resolution gives better ratios for gray/white, white/ventricles, and gray/ventricles regardless of which reconstruction algorithm is used. These results are consistent with those of simulation studies and phantom studies.[4,5] Muehllehner[4] found that the number of counts could be reduced by a factor of four for a 2 mm improvement in spatial resolution over a wide range of parameters. For example, in this study the UHRF gave better image quality and a better contrast ratio than the HRF with an improvement in resolution by 2 mm and with a 50% sensitivity. Our results show that improvement in resolution by 1–2 mm for both parallel-hole and fan-beam collimators leads to an improvement in image quantitation as well as image quality.

In addition, the quantitative approach with SPECT for estimating the regional concentration of radioactivity can be influenced by inaccuracies in image reconstruction. Shape- and size-dependent partial voluming effects could cause an underestimation of the gray-to-white matter ratio when compared with the true ratio of 4 to 1.[12] Using the standard Butterworth filtered backprojection, the estimated gray-to-white matter ratio was approximately 1.5 to 1 for all of four collimators (HRF, UHRF, HRP and UHRP). The Wiener filter improves the gray-to-white matter ratio up to approximately 2 to 1 by partially compensating for finite detector resolution, scatter and septal penetration, without amplifying the statistical noise.

We conclude that higher resolution collimators are preferable to higher sensitivity collimators, and fan-beam collimators are preferable to parallel-hole collimators for SPECT studies of cerebral perfusion. The results also indicate that the Wiener filter improves the gray-to-white matter contrast ratios of SPECT brain images regardless of which collimator is used to acquire the data.

ACKNOWLEDGMENTS

The authors would like to thank Dr. Hugh T. Morgan for many useful discussions.

REFERENCES

1. Pupi A, De Cristofaro MTR, Bacciottini LB, Antoniucci D, Formiconi AR, Mascalchi M, et al. An analysis of the arterial input curve for technetium-99m-HMPAO: quantification of rCBF using single-photon emission computed tomography. *J Nucl Med* 32: 1501–1506, 1991.
2. Devous MD, Payne JK, Lowe JL. Dual-isotope brain SPECT imaging with technetium-99m and iodine-123: clinical validation using xenon-133 SPECT. *J Nucl Med* 33: 1919–1924, 1992.
3. Devous MD, Payne JK, Lowe JL, Leroy RF. Comparison of technetium-99m-ECD to xenon-133 SPECT in normal controls and in patients with mild to moderate regional cerebral blood flow abnormalities. *J Nucl Med* 34: 754–761, 1993.
4. Muehllehner G. Effect of resolution on required count density in ECT imaging: a computer simulation. *Phys Med Biol* 30: 163–173, 1985.
5. Fahey FH, Harkness BA, Keyes JW Jr, Madson MT, Battisti C, Zito V. Sensitivity, resolution and image quality with a multi-head SPECT camera. *J Nucl Med* 33: 1859–1863, 1992.
6. Madson MT, Chang W, Hichwa RD. Spatial resolution and count density requirements in brain SPECT imaging. *Phys Med Biol* 37: 1625–1636, 1992.
7. Tsui BMW, Gullberg GT, Edgerton ER, Gilland DR, Perry JR, McCartney WH. Design and clinical utility of a fan beam collimator for SPECT imaging of the head. *J Nucl Med* 27: 810–819, 1986.
8. King MA, Schwinger RB, Doherty PW, Penny BC. Two-dimensional filtering of SPECT images using the Metz and Wiener filters. *J Nucl Med* 25: 1234–1240, 1984.
9. King MA, Schwinger RB, Penny BC, Doherty PW. Digital restoration of indium-111 and iodine-123 SPECT images with optimized Metz filters. *J Nucl Med* 27: 1327–1336, 1986.
10. Gilland DR, Tsui BMW, McCartney WH, Perry JR, Berg J. Determination of the optimum filter function for SPECT imaging. *J Nucl Med* 29: 643–650, 1988.
11. Gilland DR, Jaszczak RJ, Greer KL, Coleman RE. Quantitative reconstruction of iodine-123 data. *J Nucl Med* 32:

527–533, 1991.
12. Kim HJ, Zeeberg BR, Fahey FH, Hoffman EJ, Reba RC. 3D SPECT simulations of a complex 3D mathematical brain model: effects of detector response, attenuation, scatter, and statistical noise. *IEEE Trans Med Imag* 11: 176–182, 1992.
13. Atkins FB. Monte carlo analysis of photon scattering in radionuclide imaging. Ph.D. dissertation, University of Chicago, 1978.
14. Press WH, Flannery BP, Teukolsky SA, Vetterling WT. *Numerical Recipes in C: the art of scientific computing*. Cambridge, Cambridge University Press, pp. 221–223, 1988.
15. Tyson RK, Amtey SR. Practical considerations in gamma camera line spread function measurement. *Med Phys* 5: 480–484, 1978.
16. Hoffman EJ, Cutler PD, Digby WM, Mazziotta JC. 3-D phantom to simulate cerebral blood flow and metabolic images for PET. *IEEE Trans Nucl Sci* 37: 616–620, 1990.
17. King MA, Doherty PW, Schwinger RB, Penny BC. A Wiener filter for nuclear medicine images. *Med Phys* 10: 876–880, 1983.
18. Chang LT. A method for attenuation correction in radionuclide computed tomography. *IEEE Trans Nucl Sci* NS-25: 638–643, 1978.
19. Harris CC, Greer KL, Jaszczak RJ, Floyd CE Jr, Fearnow EC, Colman RE. Tc-99m attenuation coefficients in water-filled phantoms determined with gamma cameras. *Med Phys* 11: 681–685, 1984.
20. Jaszczak RJ, Floyd CE, Coleman RE. Scatter compensation techniques for SPECT. *IEEE Trans Nucl Sci* 32: 786–793, 1985.
21. Kim HJ, Smith RJ, Karp JS. Registration and relative quantitation of SPECT and PET data in neuroimaging when MRI data are used for anatomical information. *J Nucl Med* 34: 124, 1993 (abstract).